THE JOURNAL OF PHYSICAL CHEMISTRY C
A JOURNAL OF THE AMERICAN CHEMICAL SOCIETY

pubs.acs.org/JPCC

Article

Unraveling the Origins of Strong and Reversible Chemisorption of Carbon Dioxide in a Green Metal–Organic Framework

Hanh D. M. Pham and Rustam Z. Khaliullin*

Cite This: J. Phys. Chem. C 2021, 125, 24719–24727

Read Online

ACCESS | Metrics & More | Article Recommendations | Supporting Information

ABSTRACT: Cyclodextrin-derived metal–organic frameworks (MOFs) are remarkable not only because of their ability to absorb carbon dioxide strongly and reversibly but also because they can be readily obtained from inexpensive, renewable, and environmentally benign components. Despite the wealth of data on the carbon dioxide intake by CD-MOF-2, a representative of these MOFs, the nature and structural characteristics of its diverse adsorption sites, capable of binding CO_2 in the irreversible, reversible, and weak regimes, remain unclear. A comprehensive analysis of the results of the density functional theory modeling performed in this work in conjunction with experimental data shows that the hydroxyl counterions in CD-MOF-2 pull the protons away from the cyclodextrin alcohol groups, increasing their nucleophilic strength and turning them into strongly binding alkoxide chemisorption sites. At the same time, the diverse hydrogen bonding environments of the alkoxide sites reduce their nucleophilic character to a different extent, tuning their CO_2 binding to become irreversible, reversible, or weak. By linking the acid–base proton equilibrium and hydrogen bonding—two chemical concepts widely used for liquids—to the strength of the CO_2 binding in CD-MOF-2, this work suggests new strategies for advancing design of tunable solid materials for CO_2 capture or detection.

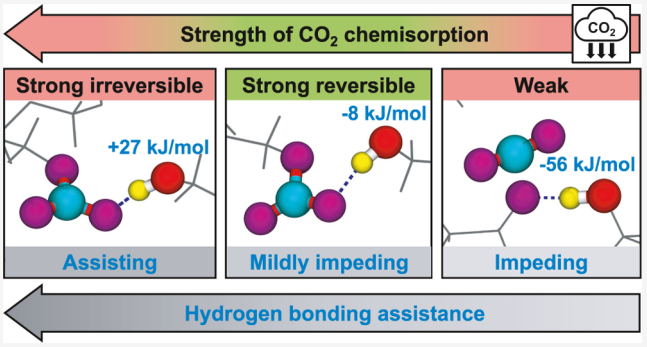

INTRODUCTION

Rising anthropogenic emission of carbon dioxide and the concomitant increase of the average global temperature[1] has created an urgent need to reduce the atmospheric levels of CO_2 or at least halt their rise.[2] Until long-term solutions to this challenge such as sunlight-driven conversion of CO_2 into fuels reach maturity, carbon dioxide capture and storage (CCS) is envisioned as an important short-term strategy to lower atmospheric CO_2 concentration. During the capture step of CCS, carbon dioxide from flue gas must be separated from other gases to create a high-purity CO_2 stream that is sequestered in the subsequent storage step. The adsorption of carbon dioxide followed by its release is proposed as one of the most reliable ways to capture CO_2 selectively. Therefore, low-cost environmentally benign materials capable of adsorbing large quantities of CO_2 fast, selectively, and reversibly are being actively sought.[3]

Physisorption of carbon dioxide—that is, CO_2 binding through weak electrostatic, hydrophobic, or van der Waals forces—has been extensively studied experimentally and computationally as a promising carbon capture procedure.[4−8] Significant research effort has also been devoted to CO_2 chemisorption—binding of carbon dioxide through stronger chemical bonds such as covalent, ionic, or metallic.[5,9−11] Because of the strong CO_2 binding, chemisorption is viewed as an important strategy to increase the adsorption capacity of materials. However, carbon dioxide is often bound too strongly in the process of chemisorption, making its release difficult and thus energetically costly. High activation barriers of chemisorption reactions often make the absorption and release slow. Fortunately, there is a variety of chemisorption reactions; the thermodynamics and kinetics of which can be tuned to the desired range.[12−17]

Metal–organic frameworks (MOFs), long known for their ability to absorb large amount of gas efficiently,[5,18,19] have recently been gaining attention as promising carbon capture materials.[20−24] While most studies of carbon capture in MOFs have focused on CO_2 physisorption, it has been found that MOFs can bind carbon dioxide chemically. In this respect, a family of MOFs based on γ-cyclodextrin[25] are of particular interest not only because of their remarkable ability to absorb carbon dioxide strongly and reversibly[26] but also because they can be synthesized from green components.[27] It has been reported that MOFs with body-centered cubic structure can be

Received: August 28, 2021
Revised: October 18, 2021
Published: November 1, 2021

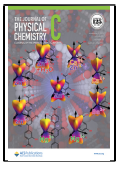

https://doi.org/10.1021/acs.jpcc.1c07610
J. Phys. Chem. C 2021, 125, 24719−24727

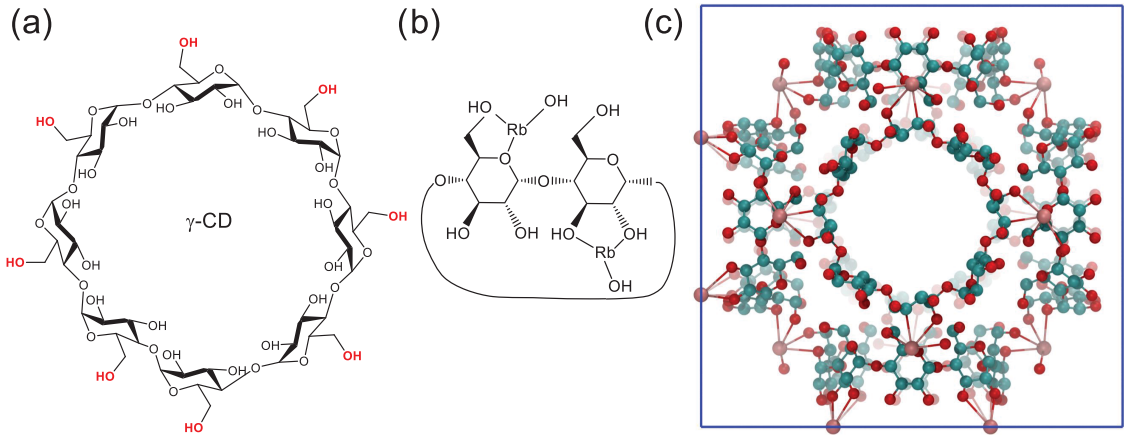

Figure 1. (a) Cyclic arrangement of γ-cyclodextrin (CD) showing eight α-1,4-linked D-glucopyranosyl residues with the primary alcohol groups colored red. (b) Repeating maltosyl unit of CD with attached rubidium ions. (c) Cubic unit cell of CD-MOF-2 with carbon, oxygen, and rubidium atoms shown with cyan, red, and pink colors, respectively. The primary faces of the six CD tori point inward, whereas the secondary faces are oriented outward. The CD tori are connected via rubidium cations, forming an extended crystal structure.[25,26,28]

crystallized at ambient temperature and pressure from the solution of γ-cyclodextrin (CD) and alkali halides in the mixture of water and ethanol[25]—substances that are inexpensive, renewable, environmentally benign, and even edible. X-ray diffraction has shown[25] that the cubic unit cell of CD-MOF-2—the γ-cyclodextrin MOF obtained using RbOH instead of halides—contains six CD units linked by rubidium ions (Figure 1).

Initial gas-uptake experiments have indicated[29,30] that the activated dry form of CD-MOF-2—with an empirical formula of the unit cell[25,29,30] given by $[(C_6H_{10}O_5)_8(RbOH)_2]_6$—absorbs CO_2 with very high selectivity over CH_4[26] and C_2H_2.[29] Because of the steep rise of the CO_2 adsorption isotherm, it has been suggested that CO_2 forms strong covalent bonds with adsorption sites in this MOF. At the same time, the color of a methyl red pH indicator diffused into the pores of CD-MOF-2 has been found to change reversibly with the application and release of CO_2 pressure, indicating that the CO_2 binding is also reversible.[26,31]

Subsequent calorimetry experiments have been used to measure the enthalpy of the CO_2 adsorption directly.[28] They have revealed that, at near-zero coverage, CO_2 is chemisorbed irreversibly with the enthalpy of −113.5 kJ/mol, whereas at higher coverage, the binding becomes reversible and the chemisorption enthalpy increases to −65.4 kJ/mol. At yet higher coverage, the weaker binding with the enthalpy of −40.1 kJ/mol has been observed and attributed to physisorbed CO_2.

With the accumulation of experimental data, it has been hypothesized[26] that CO_2 is chemisorbed by reacting with weakly nucleophilic alcohol groups on CD units and forming the alkylcarbonic adduct. This hypothesis has been supported by ^{13}C nuclear magnetic resonance (NMR) spectra of CD-MOF-2 that exhibit a new 158 ppm peak when exposed to CO_2.[26,32] The possibility of CO_2 reacting with hydroxyl counterions of CD-MOF-2 have been eliminated in control studies that use weakly basic fluoride counterions in CD-MOF-2 but still exhibit the 158 ppm peak upon exposure to CO_2. The reversibility of CO_2 uptake has been suggested as further evidence that CO_2 does not react with hydroxyl counterions since the latter process is known to be irreversible. It has also been speculated that more reactive primary alcohol groups chemisorb CO_2 stronger than the secondary groups.[26,33]

Despite the wealth of experimental data, there are multiple unanswered questions about the microscopic mechanism of the CO_2 binding in CD-MOF-2. One of the key questions is why alcohol groups, which are known to be inert to CO_2 in simple alcohols,[32] react with carbon dioxide in CD-MOF-2. It is also unclear what is the atomistic structure of adsorption sites, and if CO_2 binds exclusively to alcohol groups, why the adsorption enthalpy differs drastically for different sites. With the enormous practical importance of strong and reversible CO_2 binding, answering these fundamental questions can help modify the chemistry of MOFs and help design better materials for CCS and multiple other applications such as gas separation,[29,34] CO_2 detection in gas mixtures,[31] electrochemical sensing of CO_2,[3535] and MOF-based memristors.[36,37]

In this work, atomistic modeling of CO_2 binding in CD-MOF-2 was performed to answer these questions and advance the fundamental understanding of CO_2 chemisorption. While computational methods have been widely used to design materials that utilize the physisorption process in MOFs for CCS applications,[38−44] computational studies of chemisorption have been limited.[16,17,45] This is partially because the bond formation in chemisorption processes cannot be described with traditional force field methods and typically requires more computationally demanding electronic structure methods such as density functional theory (DFT).

■ COMPUTATIONAL MODELS AND METHODS

All calculations were performed using the DFT module of the CP2K software package.[46] The dispersion-corrected[47] generalized gradient approximation of Becke and Lee−Yang−Parr (BLYP)[48,49] was used as the exchange-correlation functional. In the dual Gaussian and plane-wave scheme implemented in CP2K,[50] double-ζ valence basis set with one set of polarization functions (DZVP)[51] and triple-ζ valence (TZV2P) with two set of polarization functions were used to represent atomic orbitals of Rb atoms and all other atoms, respectively. A plane-wave cutoff of 300 Ry was used to describe the electron density. Separable norm-conserving Goedecker−Teter−Hutter pseudopotentials were used to describe interactions between valence electrons and ionic cores.[52,53] The self-consistent field procedure was carried out using the direct minimization orbital transformation approach[54] with the kinetic preconditioner. For

https://doi.org/10.1021/acs.jpcc.1c07610
J. Phys. Chem. C 2021, 125, 24719−24727

negatively charged unit cells, calculations were done with the positive neutralizing uniform background. Atomic positions of all atoms were optimized using the limited-memory Broyden–Fletcher–Goldfarb–Shanno algorithm until the maximum force on atoms decreased below 0.00045 au.

A model of the unit cell of CD-MOF-2 was constructed using crystallographic data[55] obtained from the Cambridge Crystallographic Data Centre.[56] To reproduce partial site occupation, rubidium cations were placed randomly in a half of the available crystallographic sites. Hydroxyl counterions, the precise positions of which cannot be obtained in X-ray diffraction experiments, were coordinated on rubidium ions. Water molecules were removed to obtain a unit cell with the stoichiometric formula $[(C_6H_{10}O_5)_8(RbOH)_2]_6$ that is in agreement with the composition of the degassed CD-MOF-2 used in CO_2 adsorption experiments[25,28] Atomic positions were optimized with lattice parameters fixed at their experimental values.

In addition to performing simple geometry relaxation of the experimentally determined crystal structure of CD-MOF-2, 2 ps constant volume constant temperature ab initio molecular dynamics (AIMD) simulations were carried out at T = 400 K followed by the geometry optimization of the last AIMD snapshot. This was done to allow the thermal motion in AIMD simulations to re-arrange hydrogen bonds between the CD units of CD-MOF-2 and to produce more diverse adsorption environments.

Adsorption of carbon dioxide in CD-MOF-2 was modeled by attaching a single CO_2 molecule to the oxygen atom of a preselected alcohol group in the unit cell. The initial position of the CO_2 group was generated in internal coordinates (i.e., Z-matrix) relative to the adsorption site. The oxygen binding site (O*) and its two preceding carbons (C*) from the oligosaccharide were used as three reference atoms to specify the CO_2 internal coordinates. The initial bond length between the carbon atom of CO_2 and O* was set to 1.32 Å, whereas the C*O*C bond angle and C*C*O*C dihedral angle were drawn randomly from 125–145 and 120–360° ranges, respectively. In addition, the O*CO angle was set to 125°, while the OCO angle of the CO_2 molecule was set to 110°. These values were based on the structural experimental data for carbonic acid, which is expected to be similar to the alkylcarbonic adduct. Initial configurations with substantial interatomic overlap were rejected, and the random structure generation was repeated until a chemically reasonable adduct structure without bad interatomic contacts was obtained.

Based on the arguments outlined in the Supporting Information, the enthalpy of adsorption was approximated with the energy of adsorption.

RESULTS AND DISCUSSION

Since the precise location of hydrogen atoms at adsorption sites is not known from experiments,[25] different models for the location of protons before and after CO_2 adsorption were examined. The results obtained for each model are discussed below.

Chemisorption on Neutral Alcohol Groups. In the first model, the CO_2 molecule reacts with a neutral alcohol group. Upon adsorption, the proton of the alcohol group is transferred to protonate the newly formed alkylcarbonic acid (Figure 2a).

The adsorption energies for several primary and secondary neutral alcohol groups are summarized in Figure 3. All

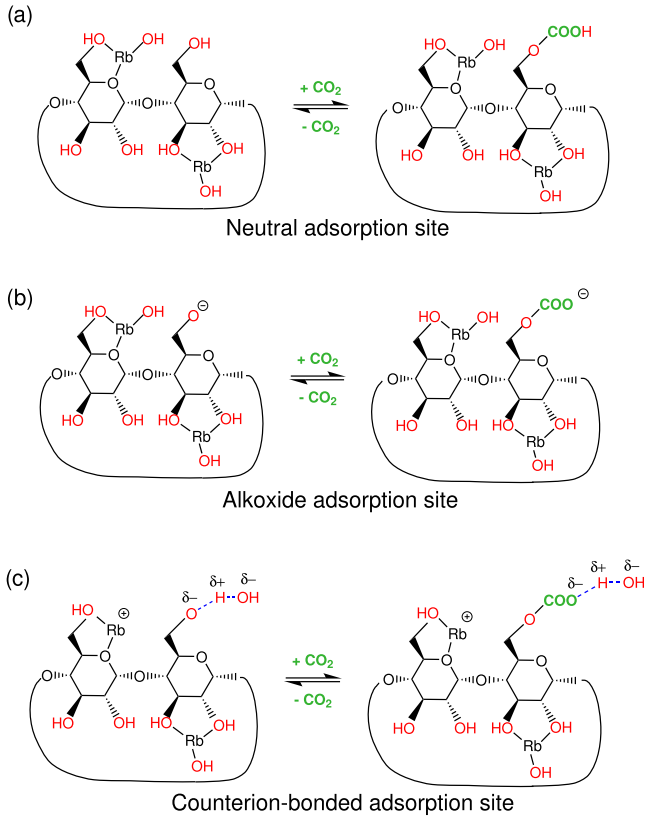

Figure 2. Model reactions for CO_2 adsorption: (a) neutral alcohol groups, (b) alkoxide groups, and (c) counterion-bonded groups. Only a single maltosyl unit of γ-cyclodextrin is shown for clarity. The proximity of CO_2 binding sites to the Rb ion in this simplified scheme might not correctly reflect the distance between them in the MOF crystal structure.

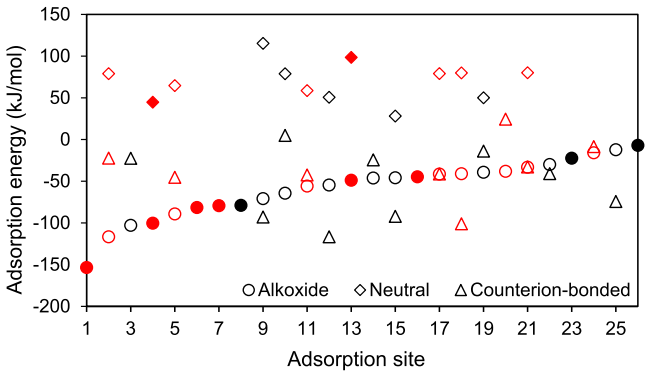

Figure 3. CO_2 adsorption energy calculated for different model reactions at primary (red) and secondary (black) binding sites. Filled shapes represent geometries generated using AIMD, whereas empty shapes represent geometries obtained from straightforward geometry optimization. The corresponding numerical data is listed in Table S1.

adsorption energies were found to be positive, lying between 28 and 115 kJ/mol. Since the entropy decreases in the adsorption process, it is clear that the formation of alkycarbonic acid via the neutral model reaction has positive free energy and, therefore, cannot proceed spontaneously contradicting experimental observations. The calculated values of the adsorption energies are also in dramatic disagreement with the experimentally measured enthalpies of adsorption lying between −114 and −40 kJ/mol.

https://doi.org/10.1021/acs.jpcc.1c07610
J. Phys. Chem. C 2021, 125, 24719–24727

Several attempts were made to search for alternative orientations of the alkylcarbonic group that could be stabilized by nearby functional groups and produce more favorable CO_2 binding. In one approach, alkylcarbonic groups were manually rotated to bring them closer to either nearby alcohol groups or nearby counterions at rubidium atoms, with the expectation that newly formed hydrogen bonds can stabilize the system. In another approach, constant volume constant temperature AIMD simulations of the combined length of 2.5 ps were performed at T = 400 K to allow thermal fluctuation to overcome low-lying energy barriers between local minima and to generate new stable configurations in an unbiased way. In both cases, the geometry of newly generated structures was reoptimized and adsorption energies were recomputed. Several structures of alkylcarbonic adducts with lower energy were found, but the reduction in the CO_2 adsorption energy was 20.3 kJ/mol on average, bringing the lowest CO_2 adsorption energy from 28.2 to 13.3 kJ/mol. This additional stabilization is not sufficient to explain the range of the experimentally measured adsorption enthalpies.

The positive adsorption energies calculated for neutral alcohol groups in CD-MOF-2 are not unexpected. They are in agreement with a body of previous studies of the interaction between CO_2 and simple alcohols.[32,57] For example, ^{1}H and ^{13}C NMR studies of pressurized CO_2 in pure anhydrous liquid methanol did not produce any evidence of the insertion of CO_2 into the O−H bond of methanol.[32] The accompanying gas-phase DFT calculations[32] showed that the standard free energy of the methylcarbonic acid formation from CO_2 and methanol is positive (41 kJ/mol) even if solvation effects are taken into account with explicitly included methanol molecules and a polarizable continuum model. Furthermore, the standard free energy of the methylcarbonic acid formation from CO_2 and methanol in the gas phase was measured to be 11 kJ/mol.[57] These measurements and calculations indicate that methylcarbonic acid is thermodynamically less stable than CO_2 and methanol. In addition to thermodynamic considerations, high-free-energy barriers have been calculated for several pathways of the methylcarbonic acid formation from CO_2 and methanol,[32] suggesting that the process is expected to be very slow.

Despite a careful account of interactions between the chemisorbed CO_2 and its environment, the failure of a neutral model to stabilize carbon dioxide in CD-MOF-2 implies that binding sites of different nature must be considered.

Chemisorption on Alkoxide Sites. To explain the strong binding of CO_2, the nucleophilic strength of a binding site was increased by the removal of the proton of a selected alcohol group, producing an alkoxide site. Although it is unclear whether these negatively charged groups exist in the real CD-MOF-2 framework, the alkoxide adsorption model depicted in Figure 2b allows estimating the maximum CO_2 binding ability of alcohol groups in CD-MOF-2. Furthermore, this simple model obviates the need to address a question of the proton location and thus enables quick exploratory calculations.

Figure 3 shows that adsorption energies for multiple randomly selected primary and secondary alkoxide sites are broadly distributed and negative. The strongest calculated binding energy (−153 kJ/mol) is stronger than the experimentally measured enthalpy for irreversible chemisorption (−114 kJ/mol), partially because of the known tendency of the employed exchange-correlation functional to overestimate binding strength (Table S2).[58,59] There are also multiple model sites with the adsorption energy matching experimentally determined ranges for reversible chemisorption (−65 kJ/mol) and physisorption (−40 kJ/mol).[28] It appears that simple alkoxide sites are capable of reproducing the range of the observed adsorption enthalpies and, therefore, can be considered as a more realistic model of CO_2 binding in CD-MOF-2 than neutral alcohol sites.

In addition to covering the range of experimentally measured interaction energies, the calculations imply that the weak CO_2 binding previously classified as physisorption can be attributed to weak chemisorption as well. Analysis of data in Figure 3 indicates that primary alkoxide sites bind CO_2 stronger (−67 ± 38 kJ/mol) than secondary sites (−47 ± 28 kJ/mol). However, the widespread of energies indicates that both primary and secondary sites can be occupied by CO_2 molecules, contrary to the previous suggestion that it is mostly primary alcohol groups that interact with carbon dioxide. It should be noted that the AIMD-generated structures of CD-MOF-2 exhibit the same ability to bind CO_2 as the structure obtained from the straightforward geometry optimization of the experimentally determined CD-MOF-2 crystal structure.

Effect of the Environment on CO_2 Adsorption. To understand the widespread of the binding energies calculated using the alkoxide model, we examined the effect of the environment on CO_2 adsorption. It can be hypothesized that the nearby alcohol groups are the primary factor affecting CO_2 binding to negatively charged sites. To verify this hypothesis, the alcohol groups located less than 3 Å from the alkoxide site were replaced by hydrogen atoms. The cutoff distance was chosen to eliminate moderate and strong hydrogen bonding interaction between the alcohol groups and the alkylcabornic adduct. As shown in Figure 4, the replacement of the alcohol

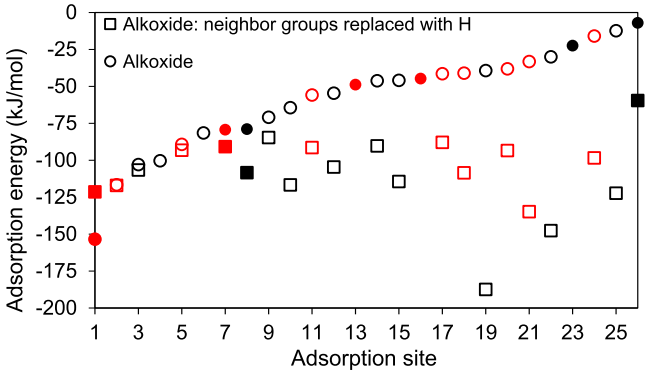

Figure 4. Effect of replacing neighbor alcohol groups with hydrogen atoms on CO_2 adsorption energies at primary (red) and secondary (black) binding sites. Filled shapes represent models using AIMD before the adsorption procedure, while the unfilled ones did not. The corresponding numerical data is listed in Table S1.

groups with hydrogen atoms results in a substantial increase in the CO_2 binding strength for most of the adsorption sites. The average adsorption energy drops from −58.2 kJ/mol for sites with alcohol neighbors to −108.5 kJ/mol for sites with hydrogen neighbors. Moreover, the spread of adsorption energies decreased from 34.6 to 26.3 kJ/mol. It was verified in a control calculation that replacing a distant alcohol group 8 Å from an alkoxide site has only a small effect (5 kJ/mol) on the adsorption energy, as expected.

Further insight into the effect of alcohol groups on the CO_2 binding strength was obtained by replacing a single nearby

https://doi.org/10.1021/acs.jpcc.1c07610
J. Phys. Chem. C 2021, 125, 24719−24727

alcohol group with a hydrogen atom. To quantify the effect of a nearby alcohol group (i) on the CO_2 adsorption energy at a given adsorption site, quantity $\Delta\Delta E_{ads}^{(i)}$ is defined

$$\Delta\Delta E_{ads}^{(i)} = \Delta E_{ads}(C^{(i)}{-}OH) - \Delta E_{ads}(C^{(i)}{-}H) \quad (1)$$

as the difference between the initial adsorption energy $\Delta E_{ads}(C^{(i)}{-}OH)$ and the adsorption energy after the substitution $\Delta E_{ads}(C^{(i)}{-}H)$. Positive values of $\Delta\Delta E_{ads}^{(i)}$ indicate that neighbor (i) weakens the CO_2 binding because CO_2 is bound more strongly after the replacement. In this case, the typically negative adsorption energy decreases upon the replacement. Conversely, a negative value of $\Delta\Delta E_{ads}^{(i)}$ indicates that neighbor (i) strengthens the CO_2 binding.

$\Delta\Delta E_{ads}^{(i)}$ values shown in Figure 5 for representative chemisorption sites indicate that nearby alcohol groups have

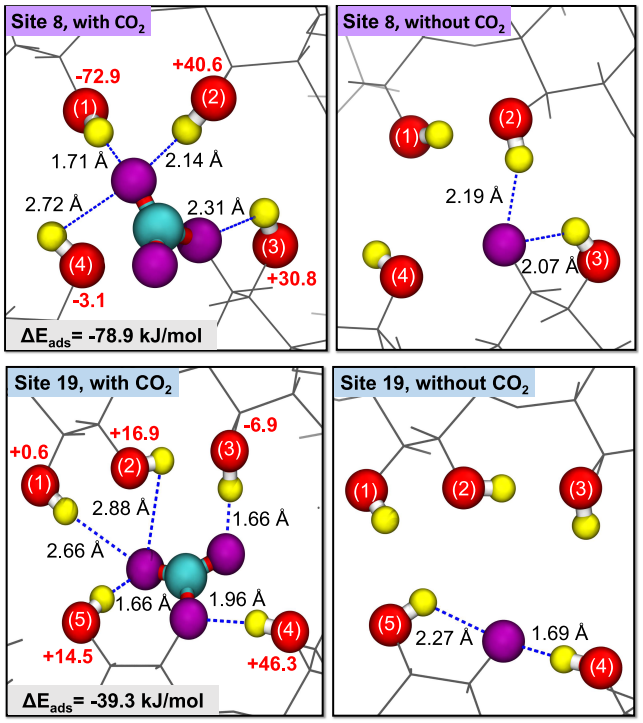

Figure 5. Effect of replacing neighbor alcohol groups with hydrogen atoms on the CO_2 binding strength. The adsorption site and nearby alcohol groups are shown as spheres in the wireframe MOF background. The CO_2 carbon atom is green and the hydrogen atoms are yellow. Oxygen atoms of the adsorption site and alkylcarbonic group are shown in purple, whereas oxygen atoms of nearby alcohol groups are shown in red. Blue dash lines represent hydrogen bonds. Values of $\Delta\Delta E_{ads}^{(i)}$, defined in eq 1, are shown as red numbers. The CO_2 adsorption energies before the neighbor replacement are shown in gray fields.

dramatically different effects on the CO_2 binding. The differences can be explained by analyzing hydrogen bonding patterns between the neighbors and the alkylcarbonic adduct (Figure 5, left panels) and also between the neighbors and the preadsorption site (Figure 5, right panels). According to the hydrogen bonds formed by the neighbors, they can be logically divided into the following three categories.

In the first category, there are alcohol groups that form hydrogen bonds with the oxygen atom of the adsorption site before and after the CO_2 adsorption. Examples of these groups include neighbor (3) of site 8 and neighbor (4) of site 19 (Figure 5). Such neighbors tend to weaken the CO_2 binding because the hydrogen bond in the preadsorption site is stronger than that in the postadsorption structure. The change in the strength of the hydrogen bond is due to the delocalization of the negative charge over the oxygen atoms in the alkylcarbonic adduct. In other words, these neighbors decrease the nucleophilic strength of the adsorption site, making its interaction with CO_2 weaker.

The second category includes alcohol groups that form hydrogen bonds with the oxygen atom of the adsorption site before the CO_2 adsorption and with the oxygen atom of CO_2 in the postadsorption structure. Neighbor (2) of site 8 and neighbor (5) of site 19 in Figure 5 are representatives of this category. The positive values of $\Delta\Delta E_{ads}^{(i)}$ for these neighbors indicate that the CO_2 insertion disrupts a stronger hydrogen bond than the hydrogen bond being formed. As a result, neighbors in this category weaken the CO_2 binding.

Alcohol groups in the third category form a hydrogen bond with the oxygen atom of CO_2 exclusively in the postadsorption alkylcarbonic structure. They make CO_2 binding stronger. The amount of stabilization depends on the geometry of the hydrogen bond that is influenced by the relative position of the bonded atoms (e.g., compare neighbors (1) and (4) of site 8 in Figure 5) and the local configuration of the hydrogen bond network that extends to the next nearest neighbors.

It is interesting to note that the sum of individual neighbor effects (Figure 5) is not equal to the combined effect of all neighbors (Figure 4). For example, the sum of effects of individual neighbors on site 8 is 1.6 kJ/mol, while their combined effect is −29.5 kJ/mol. This nonadditivity emphasizes that the insertion of CO_2 disrupts a complex network of interacting hydrogen bonds in CD-MOF-2 and the CO_2 binding is determined to some extent by the cooperativity effects in this network.

The influence of single nearby alcohol groups can also be illustrated on the example of three sites that represent adsorption sites with strong (site 1), medium (site 7), and weak (site 26) CO_2 binding energies, each lying within the three ranges described in the calorimetric studies[28] (Figure 6). As expected, the strong CO_2 chemisorption at site 1 is accompanied by the strong stabilizing effect of the neighbor

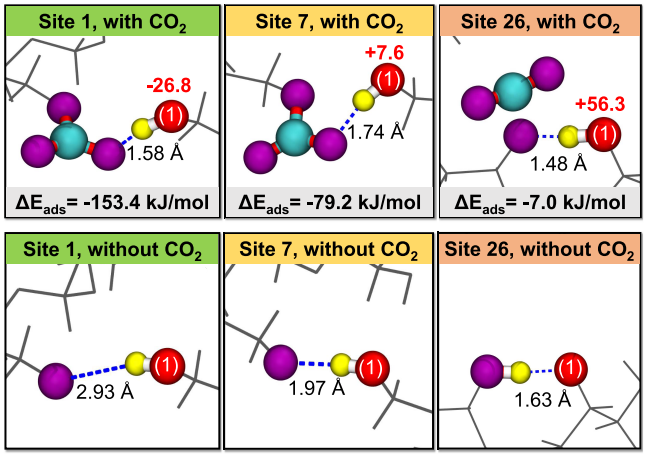

Figure 6. Effect of replacing neighbor alcohol groups with hydrogen atoms on the CO_2 binding strength for sites that bind CO_2 strongly (green), moderately (yellow), and weakly (red). Color coding and labels are explained in the caption of Figure 5.

https://doi.org/10.1021/acs.jpcc.1c07610
J. Phys. Chem. C 2021, 125, 24719−24727

from the third category. Meanwhile, the sole neighbor of the moderately binding site 7 belongs to the second category and exhibits only a minor destabilizing effect on the CO_2 adsorption. Finally, the neighbor at site 26 belongs to the first category and weakens the CO_2 adsorption dramatically. This case is a rather extreme example since the proton in the preadsorption site is completely transferred to the alkoxide site, significantly reducing its nucleophilic properties and CO_2 binding ability.

Data in Figure 6 shows that the spread in adsorption energies at the three sites is significantly reduced upon the replacement of the neighbors—an example of the general "spread-reducing" effect of the neighbor substitution seen in Figure 4. This indicates that unique hydrogen bonding environments of adsorption sites are largely responsible for their ability to bind CO_2 and for the large spread in the experimentally measured binding enthalpies. Additionally, the quantitative analysis of the hydrogen bonding suggests that the influence of nearby alcohol groups can only partially explain the spread in the binding strength. This is because the neighbor replacement does not produce equally strong adsorption sites. Besides immediate neighbors, there are apparently other factors that affect CO_2 adsorption. One example of such factors might include the electrostatic fields created by the MOF framework at the adsorption site.

The neighbor replacement experiment indicates that the CD-MOF-2 environment has an overall weakening effect on the CO_2 binding. The same effect can also be seen by comparing the strength of the CO_2 binding in CD-MOF-2 (Figure 3) and on the reference model sites with a minimal interaction between the alkoxide group and its environment (i.e., "environment-free" reference models): gas-phase methoxide (−169 kJ/mol), primary alkoxide sites on an amylose unit, and a γ-cyclodextrin torus (−113 and −84 kJ/mol, respectively).

Formation of Active Chemisorption Sites. The success of the alkoxide model in reproducing the range of CO_2 binding energies requires an investigation of the mechanism of the formation of negatively charged alcohol groups.

One of many plausible pathways to form a negatively charged active site is to transfer the proton of an alcohol group to a hydroxyl counterion—a site with strong basic properties. A series of exploratory calculations reveal that proton-transfer energies from an alcohol group to a counterion range from −103 to 232 kJ/mol (see Table S3). This widespread indicates that the proton transfer is affected by the immediate surroundings of both the donor and acceptor sites, which is not surprising in light of the discussion of environmental effects on the CO_2 adsorption energy. The presence of very low negative energies demonstrates that the formation of negatively charged alcohol groups is thermodynamically plausible if a proton is transferred to a hydroxyl counterion. At the same time, the range of calculated energies suggests that a quantitative description of the thermodynamics of this long-range proton transfer and, therefore, the formation of adsorption sites requires extensive studies employing AIMD, which are beyond the scope of this work and perhaps at the limit of the feasibility of modern high-cost AIMD methods.

An alternative to the long-range transfer of a proton is the local stabilization of the chemisorption site by a freely floating hydroxyl counterion, that is, a counterion not directly bonded to a rubidium cation (Figure 2c). Our calculations showed that some hydroxyl ions indeed detach from their rubidium sites during geometry optimization and AIMD simulations. Therefore, freely floating hydroxyls are expected to exist in CD-MOF-2 in noticeable concentrations. It was found that in 13 out of 17 considered counterion-bonded absorption sites (Figure 2c), the proton transfers spontaneously from the alcohol group to the counterion with the formation of the alkoxide site hydrogen bonded to the water molecule. Because of the strong nucleophilic character of the alkoxide group (see the previous section), it is not surprising that the CO_2 adsorption energies calculated for these proton-transferred sites are negative and also cover the range of the experimental values (Figure 3). It is remarkable that 3 out of the 17 counterion-bonded sites (i.e., sites 3, 5, and 22 in Figure 3), which do not undergo any proton transfer, are still capable of binding CO_2 although weakly. This indicates that a mere presence of a hydrogen bond between the counterion and adsorption site can create a CO_2 binding site with a sufficiently strong nucleophilic character. Another mechanism, through which a nearby counterion can stabilize the chemisorbed CO_2 molecule, is the proton transfer from the alkylcarbonic acid to a nearby counterion. This transfer was indeed observed in all 17 sites considered here.

Yet another possible mechanism of the formation of negatively charged adsorption sites is the self-ionization of the network of hydrogen-bonded alcohol groups, in which one neutral alcohol group transfers its proton to another neutral alcohol group, creating an alkoxide site. The 2 ps 400 K AIMD simulation and multiple geometry optimizations performed in this work did not produce such spontaneous self-ionization events. The only observed proton transfer occurred to hydroxyl counterions. While these limited calculations do not eliminate the possibility of self-ionization in the real CD-MOF-2 network, they imply that self-ionization is a less likely origin of adsorption sites than the proton transfer to hydroxyl counterions with strong basic properties.

Analysis of Computational and Experimental Data. The collected DFT data implies that hydroxyl counterions play an important role in the formation of alkoxide CO_2 adsorption sites, as shown in the counterion-bonded model in Figure 2c. While the indirect participation of hydroxyl counterions has not been considered before, this hypothesis is in agreement with all experimental studies of CO_2 binding in CD-MOF-2.

First, calorimetry measurements[28] suggest that less than 4.63 CO_2 molecules are adsorbed per unit cell of CD-MOF-2 at the pressure when all sites binding CO_2 strongly and reversibly are occupied (see the Supporting Information for details). Since the number of adsorbed CO_2 molecules is lower than the number of hydroxyl anions in the unit cell (12 hydroxyl ions), experimental data suggests that a sufficient number of hydroxyl anions is available to facilitate the adsorption of each CO_2 molecule. Hence, the indirect participation of hydroxyl anions is consistent with this experimental data.

Second, the indirect participation of hydroxyl counterions in the CO_2 binding is in agreement with the ^{13}C NMR 158 ppm peak attributed to alkylcarbonic products.[26] It should also be mentioned here that the DFT calculations alone cannot eliminate the possibility of the direct CO_2 adsorption on hydroxyl counterions because the calculated adsorption energy for these sites is found to be around −94 kJ/mol, which is similar to the adsorption energies on alkoxide sites. The NMR data, however, favors the model of indirect hydroxyl participation over the direct chemisorption on hydroxyl anions.

https://doi.org/10.1021/acs.jpcc.1c07610
J. Phys. Chem. C 2021, 125, 24719−24727

Third, replacing hydroxyl counterions with weakly basic fluoride anions in computer models still produces weak CO_2 binding and therefore agrees with control experimental studies, in which the fluoride-substituted CD-MOF-2 exhibits the same 158 ppm peak upon its exposure to CO_2.[25] It is important to note that only three out of eight fluoride-bonded adsorption sites (5, 12, and 18) have the negative CO_2 adsorption energy, ranging from −24 to −8 kJ/mol. The weak binding energy is not surprising because the nucleophilic strength of fluoride-bonded adsorption sites is expected to be much lower than that of hydroxyl-bonded sites. However, even a few sites with chemisorbed CO_2 are sufficient to produce the NMR signature of alkylcarbonic structures.

CONCLUSIONS

DFT modeling was used to examine the nature of CO_2 adsorption sites in CD-MOF-2—a green MOF with a remarkable ability to chemisorb carbon dioxide strongly and reversibly. It was found that the interaction of CO_2 with neutral alcohol groups on γ-cyclodextrin units of CD-MOF-2 is thermodynamically prohibitive. In contrast, the CO_2 adsorption on negatively charged alkoxide groups was shown to occur spontaneously with the range of computed interaction energies matching those measured experimentally.

A comprehensive analysis of environmental effects revealed that the strength of the CO_2 binding is largely determined by the hydrogen bonds formed by both the adsorption sites and the alkylcarbonic adducts with the surrounding alcohol groups. It was demonstrated that the network of hydrogen bonds between alcohol groups in CD-MOF-2 tends to reduce the nucleophilic character of alkoxide adsorption sites, weakening the CO_2 binding and making it reversible. The diversity of hydrogen bonding environments is also at the origins of the wide range of the adsorption energies measured for this unique MOF.

The calculations suggest that a negative alkoxide site can form readily through the proton transfer from an alcohol group to a freely floating hydroxyl counterion. The formation of a strong hydrogen bond between an alcohol group and a nearby hydroxyl counterion appears to be sufficient to chemisorb CO_2 weakly. Such indirect participation of hydroxyl counterions in the chemisorption of CO_2 was shown to be consistent with the available experimental data.

Remarkably, the calculations suggest that both primary and secondary sites bind CO_2 molecules, contrary to the previous suggestion that it is mostly primary alcohol groups that interact with carbon dioxide. The DFT data also suggests that the weak CO_2 binding previously classified as physisorption can also be attributed to weak chemisorption.

It should be noted that future computational studies aimed at a quantitative statistical description of the CO_2 binding in CD-MOF-2 should employ accelerated AIMD simulations to determine the most favorable locations of protons within the complex network of hydrogen bonds in this MOF. The utilization of hybrid density functionals can also improve the description of the energetics of the CO_2 binding. Unfortunately, such resource-demanding simulations are beyond the capabilities of most computing platforms today.

Several findings presented in this work have implications for advancing the design of materials for carbon capture and storage. By quantifying the influence of hydrogen bonds on the energetics of the CO_2 binding, this work allows estimating to which extent the carbon intake can be manipulated through hydrogen bonding. The importance of counterions for the CO_2 binding in CD-MOF-2 suggests a new strategy to tune the strength of the CO_2 chemisorption in similar "dual-agent" binding systems containing an adsorption site and activating counterion. In addition to modifying adsorption sites, changing the nature of activating agents can help to tune the CO_2 binding strength to the desired range.

ASSOCIATED CONTENT

Supporting Information

The Supporting Information is available free of charge at https://pubs.acs.org/doi/10.1021/acs.jpcc.1c07610.

Calculation of the enthalpy of adsorption, the CO_2 adsorption energy calculated for different model reactions, comparison of the CO_2 binding strength obtained with BLYP and HSE06 functionals, the energy of proton transfer from adsorption sites to hydroxyl counterions, and calculation of the number of CO_2 molecules adsorbed per unit cell of CD-MOF-2 (PDF)

AUTHOR INFORMATION

Corresponding Author

Rustam Z. Khaliullin − *Department of Chemistry, McGill University, Montreal, Quebec H3A 0B8, Canada;* orcid.org/0000-0002-9073-6753; Email: rustam.khaliullin@mcgill.ca

Author

Hanh D. M. Pham − *Department of Chemistry, McGill University, Montreal, Quebec H3A 0B8, Canada*

Complete contact information is available at: https://pubs.acs.org/10.1021/acs.jpcc.1c07610

Notes

The authors declare no competing financial interest.

ACKNOWLEDGMENTS

The research was funded by the Natural Sciences and Engineering Research Council of Canada (NSERC) through Discovery Grant (RGPIN-2016-0505) and by Tri-agency Institutional Programs Secretariat through New Frontiers in Research Fund (NFRFE-2018-00852). The authors are grateful to Compute Canada for computer resources allocated under the CFI John R. Evans Leaders Fund program.

REFERENCES

(1) *Climate Change 2014: Synthesis Report. Contribution of Working Groups I, II and III to the Fifth Assessment Report of the Intergovernmental Panel on Climate Change*; The Core Writing Team IPCC, 2015; p 151.

(2) Friedlingstein, P.; Houghton, R. A.; Marland, G.; Hackler, J.; Boden, T. A.; Conway, T. J.; Canadell, J. G.; Raupach, M. R.; Ciais, P.; le Quéré, C. Update on CO_2 Emissions. *Nat. Geosci.* **2010**, *3*, 811−812.

(3) Patel, H. A.; Byun, J.; Yavuz, C. T. Carbon Dioxide Capture Adsorbents: Chemistry and Methods. *ChemSusChem* **2017**, *10*, 1303−1317.

(4) Poloni, R.; Smit, B.; Neaton, J. B. CO_2 Capture by Metal−Organic Frameworks with van der Waals Density Functionals. *J. Phys. Chem. A* **2012**, *116*, 4957−4964.

(5) Yu, C. H.; Huang, C. H.; Tan, C. S. A Review of CO_2 Capture by Absorption and Adsorption. *Aerosol Air Qual. Res.* **2012**, *12*, 745−769.

(6) Herm, Z. R.; Swisher, J. A.; Smit, B.; Krishna, R.; Long, J. R. Metal-Organic Frameworks as Adsorbents for Hydrogen Purification

and Precombustion Carbon Dioxide Capture. *J. Am. Chem. Soc.* **2011**, *133*, 5664−5667.
(7) Abd, A. A.; Naji, S. Z.; Hashim, A. S.; Othman, M. R. Carbon Dioxide Removal through Physical Adsorption using Carbonaceous and Non-Carbonaceous Adsorbents: A Review. *J. Environ. Chem. Eng.* **2020**, *8*, No. 104142.
(8) Müller, P.; Bucior, B.; Tuci, G.; Luconi, L.; Getzschmann, J.; Kaskel, S.; Snurr, R. Q.; Giambastiani, G.; Rossin, A. Computational Screening, Synthesis and Testing of Metal−Organic Frameworks with a Bithiazole Linker for Carbon Dioxide Capture and its Green Conversion into Cyclic Carbonates†. *Mol. Syst. Des. Eng.* **2019**, *4*, 1000−1013.
(9) D'Alessandro, D. M.; Smit, B.; Long, J. R. Carbon Dioxide Capture: Prospects for New Materials. *Angew. Chem., Int. Ed.* **2010**, *49*, 6058−6082.
(10) Fahlman, M.; Fabiano, S.; Gueskine, V.; Simon, D.; Berggren, M.; Crispin, X. Interfaces in Organic Electronics. *Nat. Rev. Mater.* **2019**, *4*, 627−650.
(11) Younas, M.; Sohail, M.; Kong, L. L.; Bashir, M. J.; Sethupathi, S. Feasibility of CO_2 Adsorption by Solid Adsorbents: A Review on Low-Temperature Systems. *Int. J. Environ. Sci. Technol.* **2016**, *13*, 1839−1860.
(12) Memon, M. Z.; Zhao, X.; Sikarwar, V. S.; Vuppaladadiyam, A. K.; Milne, S. J.; Brown, A. P.; Li, J.; Zhao, M. Alkali Metal CO_2 Sorbents and the Resulting Metal Carbonates: Potential for Process Intensification of Sorption-Enhanced Steam Reforming. *Environ. Sci. Technol.* **2017**, *51*, 12−27.
(13) Zeng, S.; Zhang, X.; Bai, L.; Zhang, X.; Wang, H.; Wang, J.; Bao, D.; Li, M.; Liu, X.; Zhang, S. Ionic-Liquid-Based CO_2 Capture Systems: Structure, Interaction and Process. *Chem. Rev.* **2017**, *117*, 9625−9673.
(14) Yang, X.; Rees, R. J.; Conway, W.; Puxty, G.; Yang, Q.; Winkler, D. A. Computational Modeling and Simulation of CO_2 Capture by Aqueous Amines. *Chem. Rev.* **2017**, *117*, 9524−9593.
(15) Radovic, L. R. The Mechanism of CO_2 Chemisorption on Zigzag Carbon Active Sites: A Computational Chemistry Study. *Carbon* **2005**, *43*, 907−915.
(16) Yu, D.; Yazaydin, A. O.; Lane, J. R.; Dietzel, P. D. C.; Snurr, R. Q. A Combined Experimental and Quantum Chemical Study of CO_2 Adsorption in the Metal-Organic Framework CPO-27 with Different Metals. *Chem. Sci.* **2013**, *4*, 3544−3556.
(17) Vaidhyanathan, R.; Iremonger, S. S.; Shimizu, G. K. H.; Boyd, P. G.; Alavi, S.; Woo, T. K. Direct Observation and Quantification of CO_2 Binding within an Amine-Functionalized Nanoporous Solid. *Science* **2010**, *330*, 650−653.
(18) Zhou, H.-C.; Long, J. R.; Yaghi, O. M. Introduction to Metal−Organic Frameworks. *Chem. Rev.* **2012**, *112*, 673−674.
(19) Poloni, R.; Lee, K.; Berger, R. F.; Smit, B.; Neaton, J. B. Understanding Trends in CO_2 Adsorption in Metal-Organic Frameworks with Open-Metal Sites. *J. Phys. Chem. Lett.* **2014**, *5*, 861−865.
(20) Rosen, A. S.; Notestein, J. M.; Snurr, R. Q. Realizing the Data-Driven, Computational Discovery of Metal-Organic Framework Catalysts, 2021. arXiv:2108.06667. https://arxiv.org/abs/2108.06667.
(21) Trickett, C. A.; Helal, A.; Al-Maythalony, B. A.; Yamani, Z. H.; Cordova, K. E.; Yaghi, O. M. The Chemistry of Metal−Organic Frameworks for CO_2 Capture, Regeneration and Conversion. *Nat. Rev. Mater.* **2017**, *2*, No. 17045.
(22) Ding, M.; Flaig, R. W.; Jiang, H. L.; Yaghi, O. M. Carbon Capture and Conversion using Metal-Organic Frameworks and MOF-Based Materials. *Chem. Soc. Rev.* **2019**, *48*, 2783−2828.
(23) Sumida, K.; Rogow, D. L.; Mason, J. A.; McDonald, T. M.; Bloch, E. D.; Herm, Z. R.; Bae, T.-H.; Long, J. R. Carbon Dioxide Capture in Metal−Organic Frameworks. *Chem. Rev.* **2012**, *112*, 724−781.
(24) Drisdell, W. S.; Poloni, R.; McDonald, T. M.; Long, J. R.; Smit, B.; Neaton, J. B.; Prendergast, D.; Kortright, J. B. Probing Adsorption Interactions in Metal−Organic Frameworks Using X-ray Spectroscopy. *J. Am. Chem. Soc.* **2013**, *135*, 18183−18190.
(25) Smaldone, R. A.; Forgan, R. S.; Furukawa, H.; Gassensmith, J. J.; Slawin, A. M.; Yaghi, O. M.; Stoddart, J. F. Metalorganic Frameworks from Edible Natural Products. *Angew. Chem., Int. Ed.* **2010**, *49*, 8630−8634.
(26) Gassensmith, J. J.; Furukawa, H.; Smaldone, R. A.; Forgan, R. S.; Botros, Y. Y.; Yaghi, O. M.; Stoddart, J. F. Strong and Reversible Binding of Carbon Dioxide in a Green Metal-Organic Framework. *J. Am. Chem. Soc.* **2011**, *133*, 15312−15315.
(27) Rajkumar, T.; Kukkar, D.; Kim, K. H.; Sohn, J. R.; Deep, A. Cyclodextrin-Metal−Organic Framework (CD-MOF): From Synthesis to Applications. *J. Ind. Eng. Chem.* **2019**, *72*, 50−66.
(28) Wu, D.; Gassensmith, J. J.; Gouveîa, D.; Ushakov, S.; Stoddart, J. F.; Navrotsky, A. Direct Calorimetric Measurement of Enthalpy of Adsorption of Carbon Dioxide on CD-MOF-2, a Green Metal-Organic Framework. *J. Am. Chem. Soc.* **2013**, *135*, 6790−6793.
(29) Li, L.; Wang, J.; Zhang, Z.; Yang, Q.; Yang, Y.; Su, B.; Bao, Z.; Ren, Q. Inverse Adsorption Separation of CO_2/C_2H_2 Mixture in Cyclodextrin-Based Metal-Organic Frameworks. *ACS Appl. Mater. Interfaces* **2019**, *11*, 2543−2550.
(30) Forgan, R. S.; Smaldone, R. A.; Gassensmith, J. J.; Furukawa, H.; Cordes, D. B.; Li, Q.; Wilmer, C. E.; Botros, Y. Y.; Snurr, R. Q.; Slawin, A. M.; Stoddart, J. F. Nanoporous Carbohydrate Metal-Organic Frameworks. *J. Am. Chem. Soc.* **2012**, *134*, 406−417.
(31) Yan, T. K.; Nagai, A.; Michida, W.; Kusakabe, K.; Yusup, S. B. Crystal Growth of Cyclodextrin-based Metal-organic Framework for Carbon Dioxide Capture and Separation. *Procedia Eng.* **2016**, *148*, 30−34.
(32) Dibenedetto, A.; Aresta, M.; Giannoccaro, P.; Pastore, C.; Pápai, I.; Schubert, G. On the Existence of the Elusive Monomethyl Ester of Carbonic Acid $[CH_3OC(O)OH]$ at 300 K: ^{1}H- and ^{13}C NMR Measurements and DFT Calculations. *Eur. J. Inorg. Chem.* **2006**, *2006*, 908−913.
(33) Boger, J.; Corcoran, R. J.; Lehn, J. Cyclodextrin Chemistry. Selective Modification of All Primary Hydroxyl Groups of α- and β-cyclodextrins. *Helv. Chim. Acta* **1978**, *61*, 2190−2218.
(34) Liu, B.; Smit, B. Comparative Molecular Simulation Study of CO_2/N_2 and CH_4/N_2 Separation in Zeolites and Metal-Organic Frameworks. *Langmuir* **2009**, *25*, 5918−5926.
(35) Gassensmith, J. J.; Kim, J. Y.; Holcroft, J. M.; Farha, O. K.; Fraser Stoddart, J.; Hupp, J. T.; Jeong, N. C. A Metal-Organic Framework-Based Material for Electrochemical Sensing of Carbon Dioxide. *J. Am. Chem. Soc.* **2014**, *136*, 8277−8282.
(36) Liu, Z.; Stoddart, J. F. Extended Metal-Carbohydrate Frameworks. *Pure Appl. Chem.* **2014**, *86*, 1323−1334.
(37) Yoon, S. M.; Warren, S. C.; Grzybowski, B. A. Storage of Electrical Information in Metal-Organic-Framework Memristors. *Angew. Chem., Int. Ed.* **2014**, *53*, 4437−4441.
(38) Boyd, P. G.; Chidambaram, A.; García-Díez, E.; Ireland, C. P.; Daff, T. D.; Bounds, R.; Gładysiak, A.; Schouwink, P.; Moosavi, S. M.; Maroto-Valer, M. M.; et al. Data-Driven Design of Metal−Organic Frameworks for Wet Flue Gas CO_2 Capture. *Nature* **2019**, *576*, 253−256.
(39) Güçlü, Y.; Erer, H.; Demiral, H.; Altintas, C.; Keskin, S.; Tumanov, N.; Su, B.-L.; Semerci, F. Oxalamide-Functionalized Metal Organic Frameworks for CO_2 Adsorption. *ACS Appl. Mater. Interfaces* **2021**, *13*, 33188−33198.
(40) Burner, J.; Schwiedrzik, L.; Krykunov, M.; Luo, J.; Boyd, P. G.; Woo, T. K. High-Performing Deep Learning Regression Models for Predicting Low-Pressure CO_2 Adsorption Properties of Metal-Organic Frameworks. *J. Phys. Chem. C* **2020**, *124*, 27996−28005.
(41) Vaidhyanathan, R.; Iremonger, S. S.; Shimizu, G. K. H.; Boyd, P. G.; Alavi, S.; Woo, T. K. Competition and Cooperativity in Carbon Dioxide Sorption by Amine-Functionalized Metal−Organic Frameworks. *Angew. Chem., Int. Ed.* **2012**, *51*, 1826−1829.
(42) Queen, W. L.; Hudson, M. R.; Smit, B.; Neaton, J. B.; Long, J. R.; Brown, C. M.; Bloch, E. D.; Mason, J. A.; Gonzalez, M. I.; Lee, J. S.; et al. Comprehensive Study of Carbon Dioxide Adsorption in the Metal−Organic Frameworks M2(dobdc) (M = Mg, Mn, Fe, Co, Ni, Cu, Zn). *Chem. Sci.* **2014**, *5*, 4569−4581.

https://doi.org/10.1021/acs.jpcc.1c07610
J. Phys. Chem. C 2021, 125, 24719−24727

(43) McDonald, T. M.; Mason, J. A.; Kong, X.; Bloch, E. D.; Gygi, D.; Dani, A.; Crocellá, V.; Giordanino, F.; Odoh, S. O.; Drisdell, W. S.; et al. Cooperative Insertion of CO_2 in Diamine-Appended Metal-Organic Frameworks. *Nature* **2015**, *519*, 303−308.
(44) Yu, J.; Xie, L. H.; Li, J. R.; Ma, Y.; Seminario, J. M.; Balbuena, P. B. CO_2 Capture and Separations using MOFs: Computational and Experimental Studies. *Chem. Rev.* **2017**, *117*, 9674−9754.
(45) Forse, A. C.; Milner, P. J.; Lee, J. H.; Redfearn, H. N.; Oktawiec, J.; Siegelman, R. L.; Martell, J. D.; Dinakar, B.; Porter-Zasada, L. B.; Gonzalez, M. I.; et al. Elucidating CO_2 Chemisorption in Diamine-Appended Metal-Organic Frameworks. *J. Am. Chem. Soc.* **2018**, *140*, 18016−18031.
(46) Kühne, T. D.; Iannuzzi, M.; Del Ben, M.; Rybkin, V. V.; Seewald, P.; Stein, F.; Laino, T.; Khaliullin, R. Z.; Schütt, O.; Schiffmann, F.; et al. CP2K: An Electronic Structure and Molecular Dynamics Software Package − Quickstep: Efficient and Accurate Electronic Structure Calculations. *J. Chem. Phys.* **2020**, *152*, No. 194103.
(47) Grimme, S.; Antony, J.; Ehrlich, S.; Krieg, H. A Consistent and Accurate Ab Initio Parametrization of Density Functional Dispersion Correction (DFT-D) for the 94 Elements H-Pu. *J. Chem. Phys.* **2010**, *132*, No. 154104.
(48) Becke, A. D. Density-Functional Exchange-Energy Approximation with Correct Asymptotic Behavior. *Phys. Rev. A* **1988**, *38*, 3098−3100.
(49) Lee, C.; Yang, W.; Parr, R. G. Development of the Colle-Salvetti Correlation-Energy Formula into a Functional of the Electron Density. *Phys. Rev. B* **1988**, *37*, 785−789.
(50) Hutter, J.; Iannuzzi, M.; Schiffmann, F.; Vandevondele, J. Cp2k: Atomistic Simulations of Condensed Matter Systems. *Wiley Interdiscip. Rev. Comput. Mol. Sci.* **2014**, *4*, 15−25.
(51) VandeVondele, J.; Hutter, J. Gaussian Basis Sets for Accurate Calculations on Molecular Systems in Gas and Condensed Phases. *J. Chem. Phys.* **2007**, *127*, No. 114105.
(52) Goedecker, S.; Teter, M.; Hutter, J. Separable Dual-Space Gaussian Pseudopotentials. *Phys. Rev. B* **1996**, *54*, No. 1703.
(53) Krack, M. Pseudopotentials for H to Kr Optimized for Gradient-Corrected Exchange-Correlation Functionals. *Theor. Chem. Acc.* **2005**, *114*, 145−152.
(54) VandeVondele, J.; Hutter, J. An Efficient Orbital Transformation Method for Electronic Structure Calculations. *J. Chem. Phys.* **2003**, *118*, 4365.
(55) Smaldone, R. A.; Furukawa, J. H.; Gassensmith, J. J.; Slawin, O.; Yaghi, O. M.; Stoddart, J. F. CCDC 773710: Experimental Crystal Structure Determination. *Cambridge Crystallographic Data Centre (CCDC)*, 2011 https://www.ccdc.cam.ac.uk/.
(56) Groom, C. R.; Bruno, I. J.; Lightfoot, M. P.; Ward, S. C. The Cambridge Structural Database. *Acta Crystallogr., Sect. B: Struct. Sci. Cryst. Eng. Mater.* **2016**, *72*, 171−179.
(57) Hemmaplardh, B.; King, A. D. Solubility of Methanol in Compressed Nitrogen, Argon, Methane, Ethylene, Ethane, Carbon Dioxide, and Nitrous Oxide. Evidence for Association of Carbon Dioxide with Methanol in the Gas Phase. *J. Phys. Chem. A* **1972**, *76*, 2170−2175.
(58) Dronskowski, R. *Computational Chemistry of Solid State Materials: A Guide for Materials Scientists, Chemists, Physicists and Others*; Wiley-VCH: Germany, 2005.
(59) Sun, J.; Remsing, R. C.; Zhang, Y.; Sun, Z.; Ruzsinszky, A.; Peng, H.; Yang, Z.; Paul, A.; Waghmare, U.; Wu, X.; Klein, M. L.; Perdew, J. P. Accurate First-Principles Structures and Energies of Diversely Bonded Systems from an Efficient Density Functional. *Nat. Chem.* **2016**, *8*, 831−836.

https://doi.org/10.1021/acs.jpcc.1c07610
J. Phys. Chem. C 2021, 125, 24719−24727